Molecular Pharmacology Fast Forward. Published on June 21, 2007 as doi:10.1124/mol.107.037796
This article has not been copyedited and formatted. The final version may differ from this version.

A key role for diacylglycerol lipase-α in metabotropic glutamate receptor-dependent endocannabinoid mobilization

Kwang-Mook Jung, Giuseppe Astarita, Chenggang Zhu, Matthew Wallace, Ken Mackie, and Daniele Piomelli

Department of Pharmacology (K.M.J., G.A., D.P.) and Department of Biological Chemistry (C.Z., D.P.), University of California, Irvine, California; Department of Drug Discovery and Development, Italian Institute of Technology, Genova, Italy (D.P.); Department of Anesthesiology, University of Washington, Seattle, Washington (M.W., K.M.)

Molecular Pharmacology Fast Forward. Published on June 21, 2007 as DOI: 10.1124/mol.107.037796
This article has not been copyedited and formatted. The final version may differ from this version.

Running Title: Role of DGL-α in mGlu receptor-induced 2-AG signaling

Correspondence should be sent to:

Dr. Daniele Piomelli,

Department of Pharmacology, 3101 Gillespie NRF, University of California, Irvine, CA 92697-4625. E-mail: piomelli@uci.edu

Manuscript information:

Text pages: 30

Tables: 3 Scheme: 1 Figures: 7

References: 35 Abstract: 243 words

Introduction: 633 words Discussion: 909 words

Abbreviations:

2-AG, 2-arachidonoylglycerol; CC, coiled-coil; CNS, central nervous system; DAG, 1,2-diacylglycerol; DGL, diacylglycerol lipase; DHDG, diheptadecanoyl-*sn*-glycerol; DHPG, (*S*)-3,5-dihydroxyphenylglycine; DMEM, Dulbecco's Modified Eagle's Medium; DSI, depolarization-induced suppression of inhibition; ESI, electrospray ionization; FBS, fetal bovine serum; HDA, heptadecanoic acid; HDG, 1(3)-heptadecanoyl-*sn*-glycerol; LC/MS, liquid chromatography/mass spectrometry; MAG, monoacylglycerol; MGL, monoacylglycerol lipase; mGlu, metabotropic glutamate; PBS, phosphate-buffered saline; PCR, polymerase chain reaction; PLC, phospholipase C; RNAi, RNA interference; SAG, 1-stearoyl, 2-arachidonoyl-*sn*-glycerol; SDS-PAGE, sodium dodecylsulfate-polyacrylamide gel electrophoresis; shRNA, small-hairpin RNA; SIM, selected-ion monitoring.

Abstract

Activation of group-I metabotropic glutamate (mGlu) receptors recruits the endocannabinoid system to produce both short- and long-term changes in synaptic strength in many regions of the brain. Although there is evidence that the endocannabinoid 2-arachidonoylglycerol (2-AG) mediates this process, the molecular mechanism underlying 2-AG mobilization remains unclear. In the present study, we used a combination of genetic and targeted lipidomic approaches to investigate the role of the postsynaptic membrane-associated lipase, diacylglycerol lipase type-α (DGL-α), in mGlu receptor-dependent 2-AG mobilization. DGL-α overexpression in mouse neuroblastoma Neuro-2a cells increased baseline 2-AG levels. This effect was accompanied by enhanced utilization of the 2-AG precursor 1-stearoyl,2-arachidonoyl-*sn*-glycerol and increased accumulation of the 2-AG breakdown product arachidonic acid. A similar, albeit less marked response was observed with other unsaturated and polyunsaturated monoacylglycerols, 1,2-diacylglycerols and fatty acids. Silencing of DGL-α by RNA interference elicited opposite lipidomic changes to those of DGL-α overexpression, and abolished group-I mGlu receptor-dependent 2-AG mobilization. Coimmunoprecipitation and site-directed mutagenesis experiments revealed that DGL-α interacts, *via* a PPxxF domain, with the coiled-coil (CC)-Homer proteins Homer-1b and Homer-2, two components of the molecular scaffold that enables group-I mGlu signaling. DGL-α mutants that do not bind Homer maintained their ability to generate 2-AG in intact cells, but failed to associate with the plasma membrane. The findings indicate that DGL-α mediates group-I mGlu receptor-induced 2-AG mobilization. They further suggest that the interaction of CC-Homer with DGL-α is necessary for appropriate function of this lipase.

Molecular Pharmacology Fast Forward. Published on June 21, 2007 as DOI: 10.1124/mol.107.037796
This article has not been copyedited and formatted. The final version may differ from this version.

Introduction

The endocannabinoids are a family of lipid-derived messengers that are involved in a variety of short-range signaling events in the brain (for review, see Piomelli, 2003). Physiological experiments suggest that these lipid mediators may be released from postsynaptic neurons, diffuse across the synaptic cleft, and bind to CB_1 cannabinoid receptors on presynaptic terminals to regulate calcium and potassium channel activities, and inhibit neurotransmitter release (for review, see Freund et al., 2003; Chevaleyre et al., 2006). This retrograde signaling process appears to be widespread in the central nervous system (CNS), but two instances of its occurrence have attracted most attention. The first is a form of short-term synaptic plasticity, termed depolarization-induced suppression of inhibition (DSI), in which depolarization of a postsynaptic cell induces the transient suppression of neurotransmitter release from GABAergic nerve terminals contacting that cell (for review, see Alger, 2002; Freund et al., 2003; Chevaleyre et al., 2006). There is ample evidence that DSI – along with its counterpart at excitatory synapses, DSE – is mediated through the Ca^{2+}-dependent mobilization of an endocannabinoid messenger; however, the chemical identity of this compound remains unclear (Chevaleyre et al., 2006; Szabo et al., 2006). Another important form of endocannabinoid-mediated retrograde signaling is initiated by postsynaptic G_q-coupled receptors. In the hippocampus and other brain regions, activation of group-I metabotropic glutamate receptors (mGlu1 and mGlu5) or cholinergic muscarinic receptors depresses inhibitory and/or excitatory neurotransmission, either transiently or persistently, through a CB_1-dependent mechanism (Chevaleyre et al., 2006). This receptor-driven form of retrograde signaling is likely due to the postsynaptic release of 2-arachidonoylglycerol (2-AG).

2-AG is the most abundant endocannabinoid substance found in the mammalian CNS (Mechoulam et al., 1995; Sugiura et al., 1995; Stella et al., 1997). It is thought to be produced through phospholipase C (PLC)-catalyzed cleavage of membrane phosphatidylinositol-4,5-bisphosphate (PIP_2) to produce 1,2-

diacylglycerol (DAG), followed by diacylglycerol lipase (DGL)-mediated hydrolysis of DAG to 2-AG (Scheme 1) (Stella et al., 1997). Newly produced 2-AG is broken down by monoacylglycerol lipase (MGL) (Dinh et al., 2002; Dinh et al., 2004; Muccioli et al., 2007), which is found in excitatory and inhibitory axon terminals (Gulyas et al., 2004). Electrophysiological studies have revealed that genetic deletion of type-β PLC or pharmacological inhibition of DGL activity each abrogates group-I mGlu receptor-induced depression of excitatory transmission in the hippocampus (Hashimotodani et al, 2005; Maejiima et al., 2005; Chevaleyre and Castillo, 2003). Biochemical experiments have further demonstrated that activation of group-I mGlu receptors, most likely mGlu5, stimulates 2-AG formation in hippocampal and corticostriatal slice cultures, and that PLC or DGL inhibitors prevent this response (Jung et al., 2005). Finally, electron microscopic studies have shown that type-α DGL (DGL-α) – the most abundant of the two DGL isoforms expressed in adult brain tissue (Bisogno et al., 2003) – is localized to dendritic spines of glutamatergic synapses throughout the hippocampus and cerebellum (Katona et al., 2006; Yoshida et al., 2006). Notably, DGL-α is concentrated in a perisynaptic compartment of the dendritic spine, which is also known to contain mGlu5 receptors (Lujan et al., 1996; Lujan et al., 1997).

To understand the functions served by 2-AG in retrograde signaling, it is essential to identify the molecular mechanism responsible for its mobilization. In the present study, we have combined genetic and targeted lipidomics approaches to explore the role of DGL-α in mGlu receptor-dependent 2-AG formation. Using the mouse neuroblastoma cell line, Neuro-2a, which constitutively expresses mGlu5 receptors, we examined whether changes in DGL-α expression alter 2-AG mobilization and influence the cellular profile of 2-AG-related lipids. We also asked whether Homer proteins containing the coiled-coil (CC) domain (Ehrengruber et al., 2004) – which are obligatory components of the postsynaptic mGlu5 receptor complex (Ango et al., 2001; Bockaert et al., 2004; Sala et al., 2005) – regulate the cellular localization and enzymatic activity of DGL-α.

Molecular Pharmacology Fast Forward. Published on June 21, 2007 as DOI: 10.1124/mol.107.037796
This article has not been copyedited and formatted. The final version may differ from this version.

Materials and Methods

Chemicals

(*S*)-3,5-Dihydroxyphenylglycine (DHPG) was purchased from Tocris (Ellisville, MO). Hexadecanoic acid, heptadecanoic acid, octadecanoic acid, Δ^{9} octadecenoic acid, $\Delta^{9,12}$ octadecadienoic acid, $\Delta^{9,12,15}$ octadecatrienoic acid, $\Delta^{8,11,14}$ eicosatrienoic acid, eicosatetraenoic acid, eicosapentaenoic acid and docosahexaenoic acid were from Nu-Chek Prep (Elysian, MN); 1(3)-palmitoyl-*sn*-glycerol, 1(3)-heptadecanoyl-*sn*-glycerol, 1(3)-stearoyl-*sn*-glycerol, 1(3)-oleoyl-*sn*-glycerol, 1(3)-linoleoyl-*sn*-glycerol, 1(3)-linolenoyl-*sn*-glycerol, 1(3)-eicosatrienoyl-*sn*-glycerol, 1(3)-arachidonoyl-*sn*-glycerol, 1(3)-docosahexaenoyl-*sn*-glycerol were from Nu-Chek Prep (Elysian, MN); 2-arachidonoyl-*sn*-glycerol, 2-linoleoyl-*sn*-glycerol from Cayman Chemicals (Ann Arbor, MI) and 2-oleoyl-*sn*-glycerol were from Sigma-Aldrich (St. Louis, MO). 1,3-Diheptadecanoyl-*sn*-glycerol from Nu-Chek Prep (Elysian, MN), 1-stearoyl,2-arachidonoyl-*sn*-glycerol, 1-stearoyl,2-linoleoyl-*sn*-glycerol, 1-oleoyl,2-palmitoyl-*sn*-glycerol, 1-palmitoyl,2-stearoyl-*sn*-glycerol, 1,2-dipalmitoyl-*sn*-glycerol, 1,2-dioleoyl-*sn*-glycerol were from Avanti Polar Lipids (Alabaster, AL). Solvents were purchased from Burdick and Jackson's (Muskegon, MI).

Plasmids

We amplified the full-length coding sequence of DGL-α by polymerase chain reaction (PCR) using High Fidelity PCR Master (Roche, Indianapolis, IN) and first-strand mouse brain cDNAs as templates. We designed two primers using sequences obtained from the NCBI database (Bisogno et al., 2003): 5'-DGL-α (5'-GTTATGCCCGGGATCGTGGTGTTCCG-3') and 3'-DGL-α (5'-GCGTGCCGAGATGACCAGGTCATCC-3'). The PCR product was subcloned into a pEF-V5/His vector by TOPO cloning (Invitrogen, Carlsbad, CA) to construct a mammalian expression vector encoding V5-tagged DGL-α. A construct encoding an enhanced green fluorescent protein (EGFP) fusion protein to the C-terminal of DGL-α was cloned in the pEGFP-N2 vector (Clontech, Mountain View, CA) using a Sal I site. Constructs encoding Homer isoforms were

Molecular Pharmacology Fast Forward. Published on June 21, 2007 as DOI: 10.1124/mol.107.037796
This article has not been copyedited and formatted. The final version may differ from this version.

cloned by PCR amplification using first-strand rat brain cDNAs as template and subsequent subcloning in pFlag-CMV vector (Stratagene) using BamHI and EcoRI site. The primers used were: For Homer1b, 5'-GAAGGATCCATGGGGAACAACCTATCTTCAGCAC-3' (sense) and 5'-GCAGAATTCTTAGCTGCATTCTAGTAGCTTGGCCAA-3' (antisense); For Homer2, 5'-GAAGGATCCATGGGAGAGCAGCCCATCTTCACC-3' (sense) and 5'-GCAGAATTCCTAGTTATCCGTGCCTAGCTTGGAGA-3' (antisense). Site-directed mutagenesis was performed using QuickChange II XL Site-Directed Mutagenesis Kit (Stratagene), following manufacturer's instructions. The primers used were: For DGL-α P975L, 5'-AATCTGGTACCCAAGCCCCTCAGGCTCTTTGCAGGATCTG-3' (sense) and 5'-CAGATCCTGCAAAGAGCCTGAGGGGCTTGGGTACCAGATT-3' (antisense); For DGL-α F978R, 5'-ACCCAAGCCCCCCAGGCTCCGTGCAGGATCTGCCGAACCC-3' (sense) and 5'-GGGTTCGGCAGATCCTGCACGGAGCCTGGGGGGCTTGGGT-3' (antisense). All constructs obtained through PCR amplifications were verified by DNA sequencing.

Cloning and screening of shRNA constructs

We generated small-hairpin RNA (shRNA) constructs that contained both a CMV promoter-driven GFP and a U6 promoter-driven shRNA expression system. The shRNAs were designed using BLOCK-iT™ RNAi Designer (https://rnaidesigner.invitrogen.com/rnaiexpress/) and the corresponding oligonucleotides were synthesized. Sense and antisense oligonucleotides were annealed and ligated into pENTR entry vector (Invitrogen), to generate U6 promoter-shRNA-Pol III terminator cassette. The oligonucleotides used were as follows: For 191i, 5'-CACCGCATCCTTCTGAGCTGTATGACGAATCATACAGCTCAGAAGGATGC-3' (top) and 5'-AAAAGCATCCTTCTGAGCTGTATGATTCGTCATACAGCTCAGAAGGATGC-3' (bottom); For 788i (alpha-i), 5'-

Molecular Pharmacology Fast Forward. Published on June 21, 2007 as DOI: 10.1124/mol.107.037796
This article has not been copyedited and formatted. The final version may differ from this version.

CACCGCTACAAAGAAGTCTGCTACTCGAAAGTAGCAGACTTCTTTGTAGC-3' (top) and 5'-AAAAGCTACAAAGAAGTCTGCTACTTTCGAGTAGCAGACTTCTTTGTAGC-3' (bottom); For 377i, 5'-CACCGCAATGACCTCACTGCTAAGACGAATCTTAGCAGTGAGGTCATTGC-3' (top) and 5'-AAAAGCAATGACCTCACTGCTAAGATTCGTCTTAGCAGTGAGGTCATTGC-3' (bottom); For LacZ-i, 5'-CACCGCTACACAAATCAGCGATTTCGAAAAATCGCTGATTTGTGTAG-3' (top) and 5'-AAAACTACACAAATCAGCGATTTTTCGAAATCGCTGATTTGTGTAGC-3' (bottom); For Unrl-i, 5'-CACCGGATATATCCCGAACTAGACACGAATGTCTAGTTCGGGATATATCC-3' (top) and 5'-AAAAGGATATATCCCGAACTAGACATTCGTGTCTAGTTCGGGATATATCC-3' (bottom). RNAi silencing was tested by western blotting and quantitative PCR using the pENTR constructs. Three different shRNA sequences were tested and one was selected for further experiments. The selected shRNA expression cassette was amplified by PCR using M13F and M13R primers containing an Mlu I overhang at both 5' and 3' ends. The PCR product was ligated into an AAV vector (pAAV-hrGFP, Stratagene) using Mlu I sites. Constructs were confirmed by DNA sequencing.

Reverse Transcriptase-PCR and quantitative PCR

We extracted total RNA with TRIzol (Invitrogen) from Neuro-2a cells (American Type Culture Collection, Manassas, VA) cultured for 3 days after transfection, and synthesized first-strand complementary DNA using Superscript II RNaseH reverse transcriptase (Invitrogen). Reverse transcription of total RNA (0.2 μg) was carried out using oligo(dT)12-18 primers for 50 min at 42°C. For the identification of endogenous DGL-α mRNA, full-length of DGL-α was amplified from the first-strand cDNA by using primers 5'-DGL-α (5'-GTTATGCCCGGGATCGTGGTGTTCCG-3') and 3'-DGL-α (5'-

Molecular Pharmacology Fast Forward. Published on June 21, 2007 as DOI: 10.1124/mol.107.037796
This article has not been copyedited and formatted. The final version may differ from this version.

GCGTGCCGAGATGACCAGGTCATCC-3'). Real-time quantitative PCR was conducted using a Mx3000P (Stratagene). We designed primer/probe sets with Primer Express software (Applied Biosystems) and mouse DGL-α sequence obtained from NCBI database (GI: 37674270). Primers and fluorogenic probes were synthesized by TIB Molbiol (Adelphia, NJ). DGL-α mRNA levels were normalized using glyceraldehyde-3-phosphate dehydrogenase as an internal standard. The primer/probe sequences for DGL-α were: forward, 5'-CCAGGCCTTTGGGCG-3'; reverse, 5'-GCCTACCACAATCAGGCCAT-3'; TaqMan probe, 5'-ACCTGGGCCGTGGAACCAAACA-3'.

Cell transfections and lipid extractions

We cultured Neuro-2a cells (passage in culture: 4-20 after purchase from American Type Culture Collection) at 37°C with 5% CO_2 in Dulbecco's Modified Eagle's Medium (DMEM) (Gibco-Invitrogen, Carlsbad, CA) supplemented with 10% fetal bovine serum (FBS; Gibco-Invitrogen) and antibiotics (100 unit/ml Penicillin G and 100 μg/ml Streptomycin; Gibco-Invitrogen). We transfected cells at approximately 30% confluence using Superfect reagent (Qiagen, Valencia, CA) and incubated them for 72 hours at 37°C with 5% CO_2 in DMEM supplemented with 10% FBS and antibiotics. In shRNA-induced silencing experiments, transfection efficiency was approximately 50%, based on GFP monitoring. We used shRNAs designed against unrelated sequences, LacZ-i and Unrl-i, as controls (Invitrogen). Cells were washed with ice-cold phosphate-buffered saline (PBS) and scraped into 1 ml of methanol/water (1:1, vol:vol). Protein concentration was measured using the BCA protein assay (Pierce, Rockford, IL). Lipids were extracted using a chloroform/methanol mixture (2:1, 1.5 ml) containing diheptadecanoyl-*sn*-glycerol (DHDG), 1(3)-heptadecanoyl-*sn*-glycerol (HDG) and heptadecanoic acid (HDA) as internal standards (100 pmoles/sample). The organic phase was collected, dried under N_2 and dissolved in methanol/chloroform (3:1) for analyses. Extraction recovery efficiencies were measured from spiked biological samples as compared to direct injection of non-extracted lipid standards into the LC/MS: DAG=72±5%, FAEs =75±3%,

Molecular Pharmacology Fast Forward. Published on June 21, 2007 as DOI: 10.1124/mol.107.037796
This article has not been copyedited and formatted. The final version may differ from this version.

FAs=95±2%.

Lipid analyses

Monoacylglycerols (MAGs)–We used an Agilent 1100-LC system coupled to a 1946A-MS detector equipped with an electrospray ionization (ESI) interface (Agilent Technologies, Inc., Palo Alto, CA). MAGs were separated on a XDB Eclipse C_{18} column (50x4.6 mm i.d., 1.8 μm, Zorbax, Agilent Technologies). They were eluted with a gradient of methanol in water (from 85% to 90% methanol in 2.0 min and 90% to 100% in 3.0 min) at a flow rate of 1.5 ml/min. Column temperature was kept at 40˚C. MS detection was in the positive ionization mode, capillary voltage was set at 3 kV and fragmentor voltage was 120V. N_2 was used as drying gas at a flow rate of 13 liters/min and a temperature of 350˚C. Nebulizer pressure was set at 60 PSI. Commercial MAGs were used as reference standards. For quantification purposes, we monitored the Na^+ adducts of the molecular ions $[M+Na]^+$ in the selected ion-monitoring (SIM) mode, using HDG (mass-to-charge ratio, *m/z* = 367) as an internal standard. Calibration curves were generated using commercial MAGs. Limit of quantification was 1.25 pmol.

Fatty acids–We used a reversed-phase XDB Eclipse C_{18} column (50x4.6 mm i.d., 1.8 μm, Zorbax, Agilent Technologies) eluted with a linear gradient from 90% to 100% of A in B for 2.5 min at a flow rate of 1.5 ml/min with column temperature at 40˚C. Mobile phase A consisted of methanol containing 0.25% acetic acid and 5 mM ammonium acetate; mobile phase B consisted of water containing 0.25% acetic acid and 5 mM ammonium acetate. ESI was in the negative mode, capillary voltage was set at 4 kV and fragmentor voltage was 100V. N_2 was used as drying gas at a flow rate of 13 liters/min and a temperature of 350˚C. Nebulizer pressure was set at 60 PSI. We used commercially available fatty acids as reference standards, monitoring deprotonated molecular ions $[M-H]^-$ in the SIM mode. HDA (*m/z* = 269) was the internal standard. Calibration curves were generated using commercial FAs. Limit of quantification was 0.5 pmol.

Molecular Pharmacology Fast Forward. Published on June 21, 2007 as DOI: 10.1124/mol.107.037796
This article has not been copyedited and formatted. The final version may differ from this version.

DAGs–We used an Agilent 1100-LC system coupled to a MS detector Ion-Trap XCT interfaced with ESI (Agilent Technologies). DAGs were separated using a reversed-phase Poroshell 300SB C_{18} column (2.1x75 mm i.d., 5 μm, Agilent). We applied a linear gradient from 60% to 100% of mobile phase A in B in 5 min at a flow rate of 1.0 ml/min with column temperature at 30˚C. Mobile phase A consisted of methanol containing 0.25% acetic acid, 5 mM ammonium acetate; mobile phase B consisted of water containing 0.25% acetic acid, 5 mM ammonium acetate. The capillary voltage was set at 4.0 kV and skimmer voltage at 40V. N_2 was used as drying gas at a flow rate of 12 liters/min, temperature at 350˚C and nebulizer pressure at 80 PSI. Helium was used as collision gas, and fragmentation amplitude was set at 1.2V. MS detection was in the positive ionization mode. DAGs were identified based on their retention times and MS^3 properties, using synthetic standards as references. Multiple reaction monitoring was used to acquire full-scan MS/MS-spectra of selected DAG ions. Extracted ion chromatograms were used to quantify each DAG by selecting appropriate precursor>product ions. DHDG (*m/z* = 619.8>349.5) was the internal standard. Calibration curves were generated using 1-stearoyl,2-arachidonoyl-*sn*-glycerol. Limit of quantification was 1 pmol.

DGL assay

We harvested Neuro-2a cells in 50 mM Tris-HCl (pH 7.0, 1 ml/dish), and homogenized them with a Dounce homogenizer on ice. Homogenates were centrifuged at 800xg for 5 min at 4°C and the resulting supernatants were used for the assay. DGL activity was measured at 37°C for 30 min in 50 mM Tris-HCl (pH 7.0) containing 0.1% Triton X-100, tissue homogenate protein (100 μg) and DHDG (50 μM) as substrate. The reactions were stopped by adding chloroform-methanol (1:1) containing [$^2H_8$]-2-AG. After centrifugation at 1,500xg at 4°C for 5 min, the organic layers were collected and dried under N_2. The residues were suspended in chloroform/methanol (1:3, 50 μl) and analyzed by high-performance liquid chromatography/mass spectrometry (LC/MS). For

Molecular Pharmacology Fast Forward. Published on June 21, 2007 as DOI: 10.1124/mol.107.037796
This article has not been copyedited and formatted. The final version may differ from this version.

quantification purposes, we monitored the reaction product HDG $[M+Na]^+$ (m/z = 367) along with standard $[^2H_8]$-2-AG (m/z = 409).

Immunostaining and western blotting

We prepared lysates from Neuro-2a cells in a buffer containing Tris-HCl (10 mM, pH 7.4), NaCl (150 mM), Triton X-100 (1%), Nonidet P-40 (0.25%), EDTA (2 mM) supplemented with a mixture of protease inhibitors (Roche). Lysates were centrifuged at 14,000 x *g* for 10 min. Proteins (20 μg) from supernatants were separated by 4-20% sodium dodecylsulfate-polyacrylamide gel electrophoresis (SDS-PAGE), transferred to PVDF membranes, and subjected to western blotting. We used the following antibodies: monoclonal anti-V5 (1:5000, Invitrogen), polyclonal anti-V5 (1:3000, Covance, Berkeley, CA), monoclonal anti-Flag M2 (1:3000, Sigma-Aldrich, St. Louis, MO), polyclonal anti-DGL-α-int (1:2000, refer (Katona et al., 2005)). We cultured Neuro-2a cells on Labtek chamber slides (Nunc, Roskilde, Denmark), fixed them and immunostained them as described (Jung et al., 2005), using monoclonal anti-Flag M2 (1:1000) and polyclonal anti-V5 (1:1000) as primary antibodies. Alexa 488-labeled anti-mouse or Alexa 546-labeled anti-rabbit secondary antibodies (1:1000, Molecular Probes, Eugene, OR) were used for detection, which was conducted using a Eclipse E600 fluorescence microscope (Nikon, Japan) equipped with a digital camera (Diagnostic Instruments, Sterling Heights, MI).

Immunoprecipitation

We lysed the cells on ice with a buffer composed of 50 mM Tris-HCl, pH 7.0, 1 mM EDTA, 150 mM NaCl, and 1% Triton X-100 supplemented with protease inhibitor mixture (Roche). The lysates were centrifuged at 14,000 x g for 10 min at 4°C and the supernatants (0.6 ml, 1 mg/ml protein) were incubated with monoclonal anti-Flag M2 antibody (1:150, Sigma-Aldrich) overnight at 4°C. The immunocomplexes were precipitated by incubation with protein G-Sepharose (40 μl, GE Healthcare, Piscataway, NJ) for 1 hr at room temperature. The immunoprecipitates were washed 5 times with buffer, eluted with SDS sample

Molecular Pharmacology Fast Forward. Published on June 21, 2007 as DOI: 10.1124/mol.107.037796
This article has not been copyedited and formatted. The final version may differ from this version.

buffer, and analyzed by western blotting.

Statistical analyses

Results are expressed as means ± SEM. Analyses were conducted with GraphPad Prism v.4.0 (GraphPad Software, San Diego, CA) and differences were considered significant if $P < 0.05$ (Student's *t*-test). For DGL-α silencing experiments shown in Figure 3, Table I and Table III, one-way analysis of variance (ANOVA) followed by Dunnett's multiple comparison test was used. Differences were considered significant if comparison with both controls gives significant changes. A representative result from at least three independent experiments was shown. N represent the number of replicates within a single experiment.

Molecular Pharmacology Fast Forward. Published on June 21, 2007 as DOI: 10.1124/mol.107.037796
This article has not been copyedited and formatted. The final version may differ from this version.

Results

DGL-α overexpression increases cellular 2-AG content

To investigate the role of DGL-α in 2-AG mobilization, we transiently overexpressed V5-His-tagged DGL-α in mouse Neuro-2a cells. We confirmed DGL-α expression using either an anti-V5 antibody (Fig. 1A, Top) or a polyclonal antibody generated against a DGL-α-GST fusion protein (Fig. 1A, middle) measuring actin as a loading control (Fig 1A, bottom). Cells transfected with DGL-α contained significantly higher 2-AG levels than did pEF vector-transfected cells ($P< 0.001$, Student's *t*-test) (Fig. 1B and Table I). Levels of other unsaturated and polyunsaturated MAGs were also elevated in Neuro-2a-DGL-α cells compared to pEF vector-transfected controls (Table I). By contrast, the cellular content of saturated MAGs remained unchanged (Table I). Notably, MAG levels in cells transfected with either the empty pEF vector or the pEF-DGL-α vector were slightly different from those of non-transfected cells (Table I): for example, 18:1 Δ^9 MAG was significantly lower in pEF-transfected cells than in non-transfected ones ($P< 0.001$, Student's *t*-test). We attribute this difference, which was consistently observed in our experiments, to changes induced by transfection with the pEF vector. These minor differences notwithstanding, 2-AG levels were significantly higher in DGL-α-transfected cells than non-transfected ones ($P< 0.001$, Student's *t*-test).

To identify the substrates utilized by DGL-α to produce 2-AG (Scheme 1), we profiled DAG species in Neuro-2a cells by LC/MS^n. Under our analytical conditions, most endogenous DAGs were eluted from the LC column with retention times of 5 to 6 min (Fig. 2A) and yielded informative fragmentation patterns by collision-induced dissociation of their Na^+ adducts (Fig. 2B). Such patterns were utilized to identify and quantify cellular 1-acyl,2-arachidonoyl-*sn*-glycerol species, which are expected to serve as metabolic precursors for 2-AG. Significant levels of 1-stearoyl,2-arachidonoyl-*sn*-glycerol (SAG) were found in unstimulated Neuro-2a cells, where this DAG species accounted for approximately 84% of all 1-acyl,2-arachidonoyl-*sn*-glycerols present (Table II).

Molecular Pharmacology Fast Forward. Published on June 21, 2007 as DOI: 10.1124/mol.107.037796
This article has not been copyedited and formatted. The final version may differ from this version.

Importantly, SAG content was significantly reduced in DGL-α-overexpressing cells, indicating an enhanced breakdown of this 2-AG precursor (Fig. 1C).

If DGL-α cleaves SAG to generate 2-AG, unesterified stearic acid should transiently accumulate in cells. Consistent with this prediction, stearic acid levels were significantly higher in Neuro-2a-DGL-α than control cells (Fig. 1D). Other fatty acids derived from the DGL-catalyzed hydrolysis of DAGs (or from other lipolytic pathways such as the MGL-catalyzed hydrolysis of MAGs) were increased by DGL-α overexpression (Table III). The results indicate that (i) DGL-α overexpression increase 2-AG levels in Neuro-2a cells; and (ii) unstimulated Neuro-2a cells contain significant amounts of preformed DAGs, which are utilized by DGL-α to produce 2-AG.

DGL-α silencing reduces cellular 2-AG content

Next, to examine whether DGL-α silencing affects 2-AG mobilization, we engineered three distinct shRNAs and screened their ability to suppress heterologous DGL-α expression in HEK-293 cells. One of the shRNAs tested, 788i (alpha-i), produced a marked decrease in DGL-α levels (Fig. 3A). This shRNA was selected for further studies. Two control shRNAs were used, each containing an oligodeoxynucleotide sequence that is not present in the mouse or human genome. The first (LacZ-i) targeted the bacterial *lacZ* gene, while the second (Unrl-i) consisted of a random sequence of nucleotides that did not match any existing sequence in the human or mouse genome.

Neuro-2a cells constitutively express detectable, albeit low levels of DGL-α mRNA (Fig. 3B). Incubation of these cells with shRNA alpha-i caused a significant decrease in DGL-α mRNA (Fig. 3C). No such effect was observed in cells transfected with the two control shRNA (Fig. 3C). DGL-α silencing lowered DGL activity (Fig. 3D) and produced an opposite set of lipidomic changes to those caused by DGL-α overexpression: it decreased cellular levels of 2-AG (Fig. 3E and Table I), increased levels of the 2-AG precursor SAG (Fig. 3F), and decreased levels of unesterified stearic acid (Fig. 3G) and other fatty acids

Molecular Pharmacology Fast Forward. Published on June 21, 2007 as DOI: 10.1124/mol.107.037796
This article has not been copyedited and formatted. The final version may differ from this version.

(Table III). By contrast, no such changes in 2-AG levels were observed in Neuro-2a cells expressing control LacZ-i shRNA (Fig. 3D-G) or Unrl-i shRNA (Fig. 3E). Thus, DGL-α activity may contribute in an important way to constitutive 2-AG mobilization in Neuro-2a cells.

DGL-α silencing impairs mGlu receptor-dependent 2-AG mobilization

Previous studies have shown that the group-I mGlu receptor agonist DHPG stimulates 2-AG formation in organotypic cultures of rat brain slices (Jung et al., 2005). A similar effect was observed in Neuro-2a cells expressing control LacZ-i shRNA (Fig. 4A) as well as non-transfected cells (data not shown). Consistent with this finding, western blot analyses demonstrated that Neuro-2a cells contain both mGlu5 receptors and PLC-β1 (Fig. 4B). Under the same conditions, no mGlu1 receptor immunoreactivity was detected (Fig. 4B). To examine whether DGL-α participates in mGlu receptor-mediated generation of 2-AG, we tested the effects of DHPG (100 μM) in Neuro-2a cells in which DGL-α had been silenced with shRNA alpha-i. DHPG did not change 2-AG content in these cells (Fig. 4A), suggesting that DGL-α is required for mGlu5 receptor-dependent 2-AG mobilization.

Subcellular localization of DGL-α

We expressed a DGL-α-GFP fusion protein in either Neuro-2a or HEK-293 cells and visualized it using fluorescence microscopy. In contrast to GFP, which was associated with the cytosol, DGL-α-GFP was primarily found on the cell surface (Fig. 5A and B). These findings confirm previous observations indicating that DGL-α is localized to the neuronal plasma membrane (Katona et al., 2006; Yoshida et al., 2006).

DGL-α interacts with CC-Homer proteins

A bioinformatics search revealed that the cytoplasmic C-terminal end of DGL-α contains the PPxxF motif, which is characteristic of Homer-binding proteins such

Molecular Pharmacology Fast Forward. Published on June 21, 2007 as DOI: 10.1124/mol.107.037796
This article has not been copyedited and formatted. The final version may differ from this version.

as mGlu1, mGlu5 or IP_3 receptors (Fig. 6A) (Brakeman et al., 1997; Xiao et al., 2000). To determine whether DGL-α interacts with CC-Homer proteins, we conducted coimmunoprecipitation studies in HEK293 cells that heterologously expressed DGL-α along with Homer-2 or Homer-1b. We found that DGL-α coimmunoprecipitates with either protein (Fig. 6B and C). As previously shown for other Homer-binding proteins (Tu et al., 1998), such coimmunoprecipitation persisted in the presence of a high concentration of the non-ionic detergent Triton X-100 (1%). Importantly, single point mutations of proline (P975L) and phenylalanine (F978R) in the PPxxF motif of DGL-α, which are known to prevent the interaction of group-I mGlu receptors with CC-Homer (Beneken et al., 2000), abolished DGL-α/Homer-1a coimmunoprecipitation (Fig. 6C), suggesting that the two proteins interact selectively through this domain.

To determine if Homer-2 colocalizes with DGL-α in cells, we visualized both proteins using fluorescent double-immunostaining. As illustrated in Fig. 7A, Homer-2 was associated with plasma membranes and endoplasmic-like structures in the cytosol. Merged images showed that DGL-α was localized to plasma membranes together with Homer-2 (Fig. 7A). In contrast, the DGL-α mutant P975L, which is unable to bind Homer (Fig. 6C), remained associated with intracellular structures (Fig. 7A).

We next asked whether CC-Homer proteins affect the ability of DGL-α to mobilize 2-AG in intact cells. Coexpression of DGL-α with Homer-1b or Homer-2 produced only small increases in cellular 2-AG content, which were not affected by the P975L mutation (Fig. 7B). We interpret these results to indicate that, in our heterologous expression system, the interaction of CC-Homer with DGL-α is required for the membrane localization of this lipase, but not for its enzymatic activity.

Molecular Pharmacology Fast Forward. Published on June 21, 2007 as DOI: 10.1124/mol.107.037796
This article has not been copyedited and formatted. The final version may differ from this version.

Discussion

Group-I mGlu receptors regulate excitatory transmission throughout the CNS by releasing a diffusible signal that leaves the dendritic spine, crosses the synaptic cleft and activates CB_1 cannabinoid receptors on adjacent glutamatergic axon terminals (for review, see Chevaleyre et al., 2006). Although biochemical and pharmacological evidence suggests that 2-AG may be the messenger – or at least one of the messengers – responsible for this receptor-operated retrograde signaling process (Jung et al., 2005; Maejima et al., 2005), many aspects of the molecular mechanism governing 2-AG mobilization remain unknown. The present findings identify DGL-α, a serine lipase localized to the plasma membrane of glutamatergic dendritic spines (Bisogno et al., 2003; Katona et al., 2006; Yoshida et al., 2006), as a key component of the enzymatic machinery responsible for mGlu receptor-dependent 2-AG mobilization. The results further show that DGL-α selectively interacts with the CC-Homer proteins, Homer-1b and Homer-2.

Group-I mGlu receptors, consisting of the mGlu 1 and mGlu 5 subtypes, are Gq-coupled receptors that are concentrated in the perisynaptic compartment of glutamatergic dendritic spines (Nusser et al., 1994; Lujan et al., 1996; Lujan et al., 1997). They stimulate PLC-β to cleave membrane PIP_2 and produce inositol-1,4,5-trisphosphate (IP_3) – which binds to IP_3 receptors and triggers calcium release from intracellular stores – and DAG – which activates a variety of intracellular targets such as protein kinase C and C-type transient receptor potential cation (TRPC) channels (Hofmann et al., 1999). Within the spine, group-I mGlu receptors combine in a multiprotein complex that includes two of their downstream signaling effectors, IP_3 receptors (Tu et al., 1998) and TRPC-1 channels (Kim et al., 2003). A polymeric scaffold of CC-Homer proteins holds this complex together and connects it to other components of the postsynaptic density (Brakeman et al., 1997).

Our RNAi experiments suggest that silencing of recombinant DGL-α expression

Molecular Pharmacology Fast Forward. Published on June 21, 2007 as DOI: 10.1124/mol.107.037796
This article has not been copyedited and formatted. The final version may differ from this version.

in Neuro-2a cells reduces total DGL activity, decreases baseline 2-AG levels, and abrogates group-I mGlu-dependent 2-AG mobilization. These results are consistent with previous studies showing that the DGL inhibitor RHC80267 prevents mGlu5-induced 2-AG formation (Jung et al., 2005), and indicate that DGL-α may be responsible for the release of this endocannabinoid messenger. Moreover, our immunoprecipitation experiments show that DGL-α selectively interacts with CC-Homer proteins. This interaction appears to be functionally important, in that single-nucleotide mutations that prevent DGL-α binding to CC-Homer also disrupt the localization of DGL-α to the plasma membrane. Although we used a transfected cell line to test our hypothesis, this result acquires significance in light of the neuroanatomical distribution of DGL-α, which is localized to the same presynaptic compartment of the dendritic spine that contains the group-I mGlu receptor complex (Katona et al., 2006; Yoshida et al., 2006; Nusser et al., 1994; Lujan et al., 1996; Lujan et al., 1997). A functional association of mGlu receptors with DGL-α would enable this lipase to become rapidly activated in response to receptor occupation, and generate significant amounts of 2-AG in close proximity to presynaptic CB_1 receptors (Katona et al., 2006; Yoshida et al., 2006). Furthermore, the localization of DGL-α may account for the differential contribution of mGlu5 and muscarinic acetylcholine receptor to endocannabinoid-mediated plasticity, as recently observed at synapses of striatal medium spiny neurons (Uchigashima et al., 2007).

The LC/MS^n analyses conducted here, which included several key substrates and products of DGL-α-catalyzed DAG hydrolysis, allowed us to obtain a broad view of the lipidomic changes induced by DGL-α overexpression or silencing. Two noteworthy points emerge from these analyses. First, unsaturated MAGs such as 2-AG and, to a minor extent, 2-oleoylglycerol, are the primary products of DGL-α activity in intact cells. This product selectivity, which was not observed in broken cell preparations (Bisogno et al., 2003), may result from the availability in intact Neuro-2a cells of substrate DAG species containing arachidonic and

Molecular Pharmacology Fast Forward. Published on June 21, 2007 as DOI: 10.1124/mol.107.037796
This article has not been copyedited and formatted. The final version may differ from this version.

oleic acid at the *sn*-2 position. Second, unstimulated Neuro-2a cells contain significant amounts of preformed DAGs, such as SAG, which may serve as 2-AG precursors. In separate experiments, we have also found high SAG levels in various regions of snap-frozen rat brain, including the amygdala (6.6 ± 0.3 nmol/g; n=3) and the cerebellum (0.6 ± 0.02 nmol/g; n=3)(Astarita and Piomelli, unpublished observations), where SAG is presumably derived from PIP_2 hydrolysis (Wenk et al., 2003). These results suggest that elevation in intracellular Ca^{2+} levels in dendritic spines might initiate 2-AG mobilization through a direct activation of DGL-α, rather than through a traditional route involving the sequential activation of PLC-β and DGL-α. Consistent with this possibility, electrophysiological experiments have shown that DHPG-induced suppression of inhibition in the hippocampus and DSI in the cerebellum is inhibited by the DGL inhibitors RHC80267 and tetrahydrolipstatin, but is not affected by the PLC inhibitor U73122 (Edwards et al., 2006; Szabo et al., 2006).

Our experiments have not addressed the possible functions served by DGL-β, a second DGL isoform present in the mammalian CNS (Bisogno et al., 2003). Clear developmental and structural differences exist between these two isoforms (Bisogno et al., 2003). Notably, DGL-β lacks the CC-Homer-binding motif present in DGL-α and, when is expressed in Neuro-2a cells it associates with intracellular structures rather than with the plasma membrane (Jung et al., unpublished observations). However, the significance of these differences to neuronal 2-AG mobilization remains to be determined. This question notwithstanding, the present results provide new evidence for a primary role of DGL-α in mGlu5 receptor-dependent 2-AG mobilization, and highlight the value of targeted lipidomic analyses in the study of brain endocannabinoid signaling.

Molecular Pharmacology Fast Forward. Published on June 21, 2007 as DOI: 10.1124/mol.107.037796
This article has not been copyedited and formatted. The final version may differ from this version.

Acknowledgements

We thank Dr. Faizy Ahmed for helpful discussion, and Christopher Stapleton and Mariam Behbehani for their invaluable experimental help. The contribution of the Agilent Technologies/University of California, Irvine Analytical Discovery Facility, Center for Drug Discovery is gratefully acknowledged.

Molecular Pharmacology Fast Forward. Published on June 21, 2007 as DOI: 10.1124/mol.107.037796
This article has not been copyedited and formatted. The final version may differ from this version.

References

Alger BE (2002) Retrograde signaling in the regulation of synaptic transmission: focus on endocannabinoids. Prog Neurobiol 68:247-286.

Ango F, Prezeau L, Muller T, Tu JC, Xiao B, Worley PF, Pin JP, Bockaert J, Fagni L (2001) Agonist-independent activation of metabotropic glutamate receptors by the intracellular protein Homer. Nature 411:962-965.

Beneken J, Tu JC, Xiao B, Nuriya M, Yuan JP, Worley PF, Leahy DJ (2000) Structure of the Homer EVH1 domain-peptide complex reveals a new twist in polyproline recognition. Neuron 26:143-154.

Bisogno T, Howell F, Williams G, Minassi A, Cascio MG, Ligresti A, Matias I, Schiano-Moriello A, Paul P, Williams EJ, Gangadharan U, Hobbs C, Di Marzo V, Doherty P (2003) Cloning of the first sn1-DAG lipases points to the spatial and temporal regulation of endocannabinoid signaling in the brain. J Cell Biol 163:463-468.

Bockaert J, Dumuis A, Fagni L, Marin P (2004) GPCR-GIP networks: a first step in the discovery of new therapeutic drugs? Curr Opin Drug Discov Devel 7:649-657.

Brakeman PR, Lanahan AA, O'Brien R, Roche K, Barnes CA, Huganir RL, Worley PF (1997) Homer: a protein that selectively binds metabotropic glutamate receptors. Nature 386:284-288.

Chevaleyre V, Castillo PE (2003) Heterosynaptic LTD of hippocampal GABAergic synapses: a novel role of endocannabinoids in regulating excitability. Neuron 38:461-472.

Chevaleyre V, Takahashi KA, Castillo PE (2006) Endocannabinoid-mediated synaptic plasticity in the CNS. Annu Rev Neurosci 29:37-76.

Dinh TP, Carpenter D, Leslie FM, Freund TF, Katona I, Sensi SL, Kathuria S, Piomelli D (2002) Brain monoglyceride lipase participating in endocannabinoid inactivation Proc Natl Acad Sci U S A 99:10819-10824.

Dinh TP, Kathuria S, Piomelli D (2004) RNA interference suggests a primary role for monoacylglycerol lipase in the degradation of the endocannabinoid 2-arachidonoylglycerol. Mol Pharmacol 66:1260-1264.

Edwards DA, Kim J, Alger BE (2006) Multiple mechanisms of endocannabinoid response initiation in hippocampus. J Neurophysiol 95:67-75.

Ehrengruber MU, Kato A, Inokuchi K, Hennou S (2004) Homer/Vesl proteins and their roles in CNS neurons. Mol Neurobiol 29:213-227.

Freund TF, Katona I, Piomelli D (2003) Role of endogenous cannabinoids in synaptic signaling. Physiol Rev 83:1017-1066.

Gulyas AI, Cravatt BF, Bracey MH, Dinh TP, Piomelli D, Boscia F, Freund TF (2004) Segregation of two endocannabinoid-hydrolyzing enzymes into pre- and postsynaptic compartments in the rat hippocampus, cerebellum and amygdala. Eur J Neurosci 20:441-458.

Hashimotodani Y, Ohno-Shosaku T, Tsubokawa H, Ogata H, Emoto K, Maejima T, Araishi K, Shin HS, Kano M (2005) Phospholipase Cbeta serves as a coincidence detector through its Ca^{2+} dependency for triggering retrograde endocannabinoid signal. Neuron 45:257-268.

Hofmann T, Obukhov AG, Schaefer M, Harteneck C, Gudermann T, Schultz

(1999) Direct activation of human TRPC6 and TRPC3 channels by diacylglycerol. Nature 397:259-263.

Jung KM, Mangieri R, Stapleton C, Kim J, Fegley D, Wallace M, Mackie K, Piomelli D (2005) Stimulation of endocannabinoid formation in brain slice cultures through activation of group I metabotropic glutamate receptors. Mol Pharmacol 68:1196-1202.

Katona I, Urban GM, Wallace M, Ledent C, Jung KM, Piomelli D, Mackie K, Freund TF (2006) Molecular composition of the endocannabinoid system at glutamatergic synapses. J Neurosci 26:5628-5637.

Kim SJ, Kim YS, Yuan JP, Petralia RS, Worley PF, Linden DJ (2003) Activation of the TRPC1 cation channel by metabotropic glutamate receptor mGluR1. Nature 426:285-291.

Lujan R, Nusser Z, Roberts JD, Shigemoto R, Somogyi P (1996) Perisynaptic location of metabotropic glutamate receptors mGluR1 and mGluR5 on dendrites and dendritic spines in the rat hippocampus. Eur J Neurosci 8:1488-1500.

Lujan R, Roberts JD, Shigemoto R, Ohishi H, Somogyi P (1997) Differential plasma membrane distribution of metabotropic glutamate receptors mGluR1 alpha, mGluR2 and mGluR5, relative to neurotransmitter release sites. J Chem Neuroanat 13:219-241.

Maejima T, Oka S, Hashimotodani Y, Ohno-Shosaku T, Aiba A, Wu D, Waku K, Sugiura T, Kano M (2005) Synaptically driven endocannabinoid release requires Ca2+-assisted metabotropic glutamate receptor subtype 1 to phospholipase Cbeta4 signaling cascade in the cerebellum. J Neurosci 25:6826-6835.

Mechoulam R, Ben-Shabat S, Hanus L, Ligumsky M, Kaminski NE, Schatz AR,

Gopher A, Almog S, Martin BR, Compton DR, Pertwee RG, Griffin G, Bayewitch M, Barg J, Vogel Z (1995) Identification of an endogenous 2-monoglyceride, present in canine gut, that binds to cannabinoid receptors. Biochem Pharmacol 50:83-90.

Muccioli GG, Xu C, Odah E, Cudaback E, Cisneros JA, Lambert DM, Lopez Rodriguez ML, Bajjalieh S, Stella N (2007) Identification of a novel endocannabinoid-hydrolyzing enzyme expressed by microglial cells. J Neurosci 27:2883-2889.

Nusser Z, Mulvihill E, Streit P, Somogyi P (1994) Subsynaptic segregation of metabotropic and ionotropic glutamate receptors as revealed by immunogold localization. Neuroscience 61:421-427.

Piomelli D (2003) The molecular logic of endocannabinoid signalling. Nat Rev Neurosci 4:873-884.

Sala C, Roussignol G, Meldolesi J, Fagni L (2005) Key role of the postsynaptic density scaffold proteins Shank and Homer in the functional architecture of Ca2+ homeostasis at dendritic spines in hippocampal neurons. J Neurosci 25:4587-4592.

Szabo B, Urbanski MJ, Bisogno T, Di Marzo V, Mendiguren A, Bar W, Freiman I. (2006) Depolarization-induced retrograde synaptic inhibition in the cerebellar cortex is mediated by 2-arachidonoylglycerol. J Physiol 577:263-280.

Stella N, Schweitzer P, Piomelli D (1997) A second endogenous cannabinoid that modulates long-term potentiation. Nature. 388:773-778.

Sugiura T, Kondo S, Sukagawa A, Nakane S, Shinoda A, Itoh K, Yamashita A, Waku K (1995) 2-Arachidonoylglycerol: a possible endogenous cannabinoid

receptor ligand in brain. Biochem Biophys Res Commun 215:89-97.

Tu JC, Xiao B, Yuan JP, Lanahan AA, Leoffert K, Li M, Linden DJ, Worley PF (1998) Homer binds a novel proline-rich motif and links group 1 metabotropic glutamate receptors with IP3 receptors. Neuron 21:717-726.

Uchigashima M, Narushima M, Fukaya M, Katona I, Kano M, Watanabe M (2007) Subcellular arrangement of molecules for 2-arachidonoyl-glycerol-mediated retrograde signaling and its physiological contribution to synaptic modulation in the striatum. J Neurosci 27:3663-3676.

Wenk MR, Lucast L, Di Paolo G, Romanelli AJ, Suchy SF, Nussbaum RL, Cline GW, Shulman GI, McMurray W, De Camilli P (2003) Phosphoinositide profiling in complex lipid mixtures using electrospray ionization mass spectrometry. Nat Biotechnol 21:813-817.

Xiao B, Tu JC, Worley PF (2000) Homer: a link between neural activity and glutamate receptor function. Curr Opin Neurobiol 10:370-374.

Yoshida T, Fukaya M, Uchigashima M, Miura E, Kamiya H, Kano M, Watanabe M (2006) Localization of diacylglycerol lipase-alpha around postsynaptic spine suggests close proximity between production site of an endocannabinoid, 2-arachidonoyl-glycerol, and presynaptic cannabinoid CB1 receptor. J Neurosci 26:4740-4751.

Molecular Pharmacology Fast Forward. Published on June 21, 2007 as DOI: 10.1124/mol.107.037796
This article has not been copyedited and formatted. The final version may differ from this version.

Footnotes

This work was supported by grants from the National Institute on Drug Abuse (DA12447 and DA12413 to D.P. and DA11322 and DA00286 to K.M.).

K.M.J. and G.A. contributed equally to this study.

Molecular Pharmacology Fast Forward. Published on June 21, 2007 as DOI: 10.1124/mol.107.037796
This article has not been copyedited and formatted. The final version may differ from this version.

Legends for Figures

Scheme 1. Proposed route for 2-AG formation and degradation in neural cells. PIP_2, phosphatidylinositol-4,5-biphosphate; PLC, phospholipase C; DAG, diacylglycerol; DGL, diacylglycerol lipase; MAG, monoacylglycerol; MGL, monoacylglycerol lipase; FA, fatty acid.

Figure 1. Overexpression of DGL-α increases 2-AG levels in Neuro-2a cells. **A**. Recombinant DGL-α expression was assessed by western blot analysis using anti-V5 (top) or anti-DGL-α (middle) antibodies. Actin (bottom) served as a loading control. Cells were transfected with pEF6 vector (V) or DGL-α (α). **B-D**. Effects of DGL-α overexpression on the levels of **B**, 2-AG; **C**, 1-stearoyl,2-arachidonoyl-*sn*-glycerol (SAG); and **D,** unesterified stearic acid (SA). See text for details of lipid measurements. **P*< 0.05, ****P*< 0.001 *vs.* pEF, Student's *t* test (n=4).

Figure 2. Identification of 1-acyl,2-arachidonoyl-*sn*-glycerol species in Neuro-2a cells. **A,** representative LC chromatogram and **B**, mass spectra of cell-derived 1-stearoyl,2-arachidonoyl-*sn*-glycerol.

Figure 3. RNAi-induced silencing of DGL-α in Neuro-2a cells. **A**. Effects of various shRNAs on DGL-α levels in HEK293 cells expressing recombinant DGL-α-V5. Cells were harvested 72 hours after transfection, and DGL-α expression was monitored by western blot analysis using an anti-V5 antibody. **B**. Representative RT-PCR demonstrating the presence of DGL-α mRNA in Neuro-2a cells. (N), Neuro-2a cells, (C), mouse brain. **C-D.** Effects of DGL-α silencing on the level of **C,** DGL-α and **D,** DGL activity in Neuro-2a cells treated with control shRNA (LacZ-i and Unrl-i) or DGL-α shRNA (alpha-i). **E-G**. Effects of DGL-α silencing on levels of **E**, 2-AG; **F**, 1-stearoyl,2-arachidonoyl-*sn*-glycerol (SAG); and **G,** unesterified stearic acid (SA). **P*< 0.05, ***P*< 0.01 *vs.* LacZ-i,

Molecular Pharmacology Fast Forward. Published on June 21, 2007 as DOI: 10.1124/mol.107.037796
This article has not been copyedited and formatted. The final version may differ from this version.

Student's *t* test (n=4).

Figure 4. DGL-α silencing attenuates mGlu receptor-dependent 2-AG mobilization. **A**. 2-AG levels in control (LacZ-i) or DGL-α-silenced (alpha-i) Neuro-2a cells incubated with fresh media containing vehicle (open bars) or DHPG (100 μM) (closed bars) for 5 min at 37°C (n=6). ***P*< 0.01, ****P*< 0.001. **B**. Western blot analysis showing the presence of mGlu5 receptor and PLC-β immunoreactivity in extracts of Neuro-2a cells. mGlu1 receptor was not detectable by this method.

Figure 5. Recombinant DGL-α localizes to the plasma membrane and endoplasmic-like structures in Neuro-2a cells (**A**) or HEK293 cells (**B**). Forty eight hours after transfection with DGL-α-pEGFP or pEGFP, cells were fixed and the nuclei were stained with DAPI (blue). Images are representative of two separate experiments.

Figure 6. DGL-α interacts with CC-Homer proteins. **A**. The C-terminal cytoplasmic tail of human (h), mouse (m), and rat (r) DGL-α contains the Homer-binding motif PPxxF. **B**, DGL-α immunoprecipitates with Homer-2. Lysates of HEK293 cells transfected with V5-tagged DGL-α and Flag-tagged Homer-2 were incubated with an anti-Flag antibody and the resulting immunoprecipitates (IP) were analyzed by western blotting using an anti-V5 antibody to visualize DGL-α, or an anti-Flag antibody to visualize Homer-2. Immunoprecipitation of Homer by the Flag antibody causes co-immunoprecipitation of DGL-α (center lane). Input shows that identical amounts of protein were provided for the immunoprecipitation in the first two lanes. **C**. Effects of point mutations in the PPxxF Homer-binding motif of DGL-α (P975L and F978R) on its ability to immunoprecipitate with Homer-1b.

Figure 7. Interaction with CC-Homer proteins is required for the cell membrane

Molecular Pharmacology Fast Forward. Published on June 21, 2007 as DOI: 10.1124/mol.107.037796
This article has not been copyedited and formatted. The final version may differ from this version.

localization of DGL-α. **A**, Localization of DGL-α and Homer-2 in Neuro-2a cells. Cells were stained using anti-Flag to visualize Flag-Homer2 (green), and anti-V5 antibody to visualize DGL-α-V5 (red). DAPI was used to stain nuclei (blue). **B**. Levels of 2-AG were measured in Neuro-2a cells coexpressing indicated DGL-α and Homer proteins. V, pCMV Vector; H1b, Homer 1b; H2, Homer2. **P*< 0.05, ***P*< 0.01 *vs.* pCMV Vector, Student's *t* test (n=6).

Molecular Pharmacology Fast Forward. Published on June 21, 2007 as DOI: 10.1124/mol.107.037796
This article has not been copyedited and formatted. The final version may differ from this version.

Table I. MAG levels (pmol/mg protein) in Neuro-2a cells following DGL-α overexpression or silencing. *P< 0.05, ***P< 0.001 *vs.* pEF, Student's *t* test (n=4); or one-way ANOVA followed by Dunnett's test (n=4).

MAG	DGLα overexpression		DGLα silencing			Non-transfected
	pEF	alpha	LacZ-i	Unrl-i	alpha-i	
16:0 (*m/z* 353)	278±8	275±4	518±23	744±36	598±55	480±28
18:0 (*m/z* 381)	51 ±9	37±2	18±2	20±1	34±5	12±2
18:1 Δ^{9} (*m/z* 379)	206±18	399±20***	430±12	570±48	445±23	461±18
18:2 $\Delta^{9,12}$ (*m/z* 377)	29±3	68±2***	34±3	40±3	42±7	46±6
18:3 $\Delta^{9,12,15}$ (*m/z* 375)	9±2	36±23	22±1	29±3	36±2	37±4
20:3 $\Delta^{8,11,14}$ (*m/z* 403)	59±7	166±5***	72±4	92±7	83±12	174±5
20:4 $\Delta^{5,8,11,14}$ (*m/z* 401)	322±23	1001±35***	325±22	327±24	223±19*	484±29
20:5 $\Delta^{5,8,11,14,17}$ (*m/z* 399)	12±1	34±1***	13±2	15±1	10±1	29±2
22:6 $\Delta^{4,7,10,13,16,19}$ (*m/z* 425)	10 ±1	23±1***	17±1	23±1	21±1	15±1

Molecular Pharmacology Fast Forward. Published on June 21, 2007 as DOI: 10.1124/mol.107.037796
This article has not been copyedited and formatted. The final version may differ from this version.

Table II. Molecular composition of 1-acyl-2-arachidonoyl-*sn*-glycerol species in non-transfected Neuro-2a cells, as assessed by ion-trap LC/MS^n analysis.

Acyl group in *sn*-1	Precursor ion $[MNa]^+$ (*m/z*)	Product ion $[M\text{-}R_2COOH]^+$ (*m/z*)	nmol/mg protein	% mol
18:0	667.8	341.5	8.8±1.5	82
18:1	665.8	339.5	1.2±0.5	11
16:0	639.8	313.5	0.53±0.06	5
22:6	711.8	385.5	0.11±0.02	1
20:4	687.8	361.5	0.085±0.003	0.8
14:0	611.8	285.5	0.021±0.003	0.2
18:2	trace	trace	-	trace

Molecular Pharmacology Fast Forward. Published on June 21, 2007 as DOI: 10.1124/mol.107.037796
This article has not been copyedited and formatted. The final version may differ from this version.

Table III. Unesterified fatty acid levels (pmol/mg protein) in Neuro-2a cells following DGL-α overexpression or silencing. **P*< 0.05, ***P*< 0.01, ****P*< 0.001 *vs.* pEF, Student's *t* test (n=4); or one-way ANOVA followed by Dunnett's test (n=4).

Fatty acid	DGLα overexpression		DGLα silencing			Non-transfected
	pEF	alpha	LacZ-i	Unrl-i	alpha-i	
16:0 (*m/z* 255)	293±7	311±11	149±3	157±5	140±3	129±4
18:0 (*m/z* 283)	414±19	487±9*	243±5	245±10	220±7	262±7
18:1 Δ^{9} (*m/z* 281)	158±1	211±6***	127±4	129±3	96±3**	121±7
18:2 $\Delta^{9,12}$ (*m/z* 279)	10±1	13±0.2*	8.0±0.3	6.6±0.3	5.1±0.2**	5.5±0.3
18:3 $\Delta^{9,12,15}$ (*m/z* 277)	0.8±0.1	0.7±0.1	0.4±0.0	0.4±0.0	0.3±0.0	0.3±0.0
20:3 $\Delta^{8,11,14}$ (*m/z* 305)	3.5±0.1	4.8 ±0.2**	3.5±0.2	3.3±0.1	2.4±0.2*$^{(*)}$	3.0±0.2
20:4 $\Delta^{5,8,11,14}$ (*m/z* 303)	11±0.5	19±0.7***	10±0.6	7.7±0.3	5.8±0.4*$^{(*)}$	6.4±0.5
20:5 $\Delta^{5,8,11,14,17}$ (*m/z* 301)	3.7±0.4	4.8±0.3	2.5±0.1	2.2±0.1	2.6±0.1	7.2±0.6
22:6 $\Delta^{4,7,10,13,16,19}$ (*m/z* 327)	0.5±0.0	0.3±0.0	0.2±0.0	0.2±0.0	0.3 ±0.0	0.3±0.0

Molecular Pharmacology Fast Forward. Published on June 21, 2007 as DOI: 10.1124/mol.107.037796
This article has not been copyedited and formatted. The final version may differ from this version.

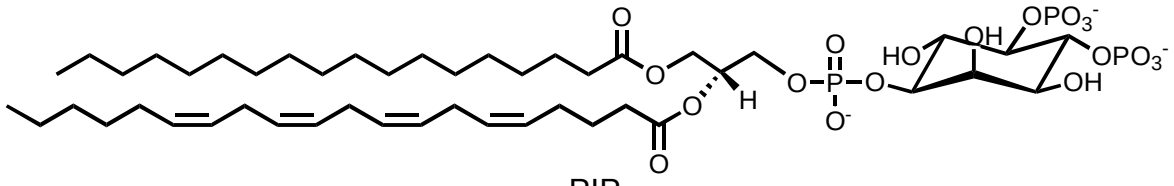

PIP_2
(1-stearoyl-2-arachidonoyl-*sn*-glycero-3-phosphoinositol-4,5-bisphosphate)

PIP_2-PLC

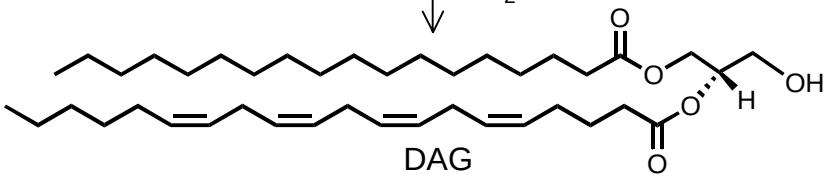

DAG
(1-stearoyl-2-arachidonoyl-*sn*-glycerol)

DGL

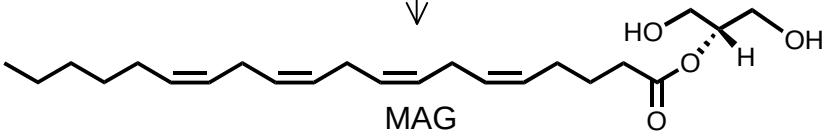

MAG
(2-arachidonoyl-*sn*-glycerol)

MGL

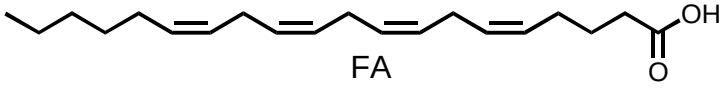

FA
(arachidonic acid)

Scheme 1

Molecular Pharmacology Fast Forward. Published on June 21, 2007 as DOI: 10.1124/mol.107.037796
This article has not been copyedited and formatted. The final version may differ from this version.

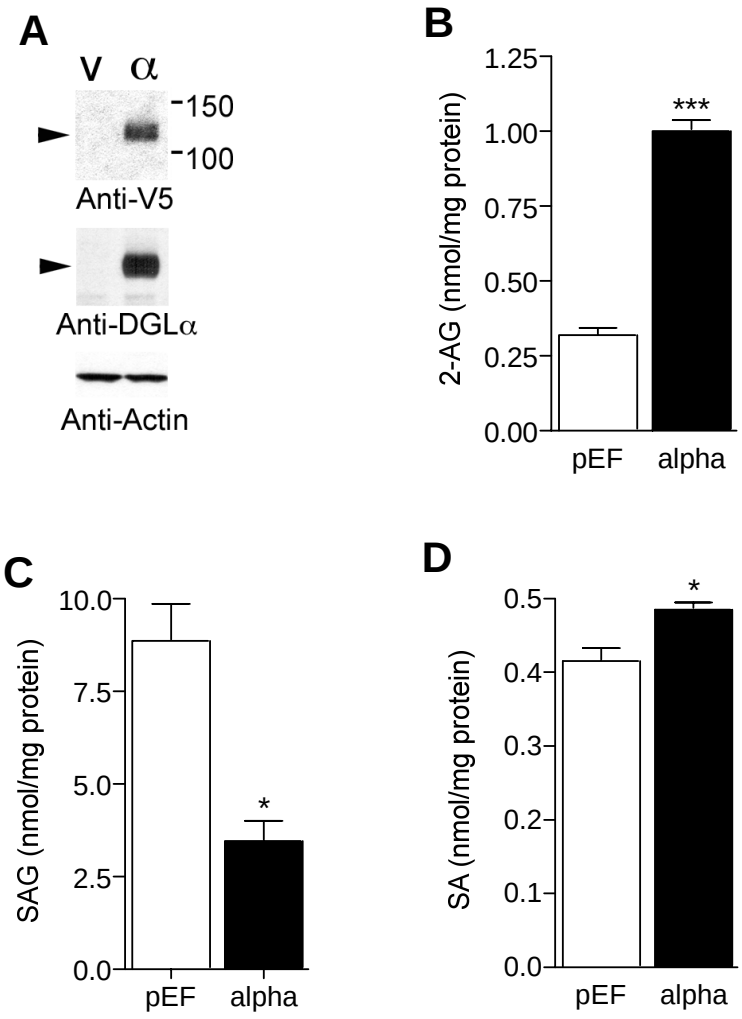

Fig 1

Molecular Pharmacology Fast Forward. Published on June 21, 2007 as DOI: 10.1124/mol.107.037796
This article has not been copyedited and formatted. The final version may differ from this version.

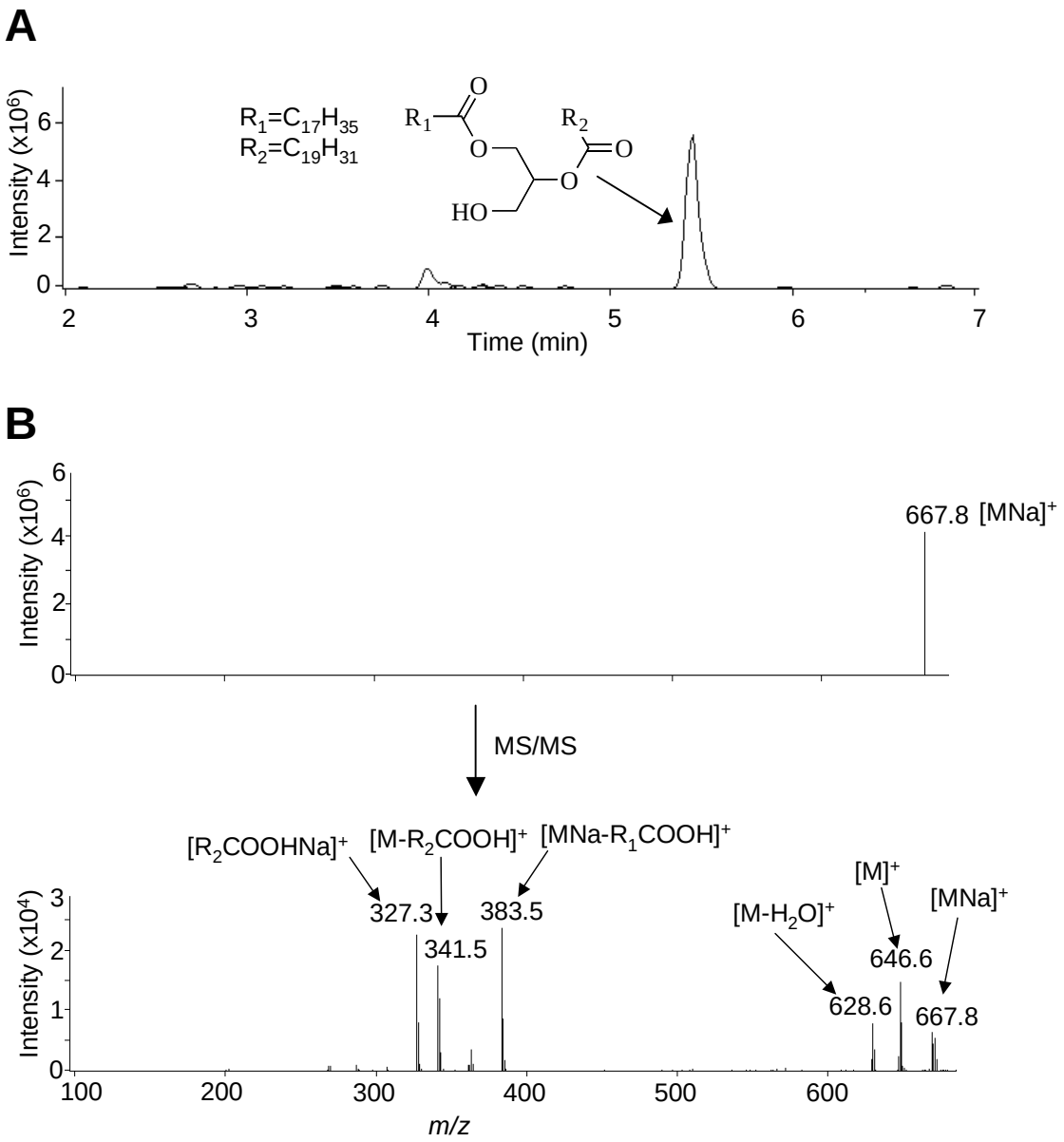

Fig 2

Molecular Pharmacology Fast Forward. Published on June 21, 2007 as DOI: 10.1124/mol.107.037796
This article has not been copyedited and formatted. The final version may differ from this version.

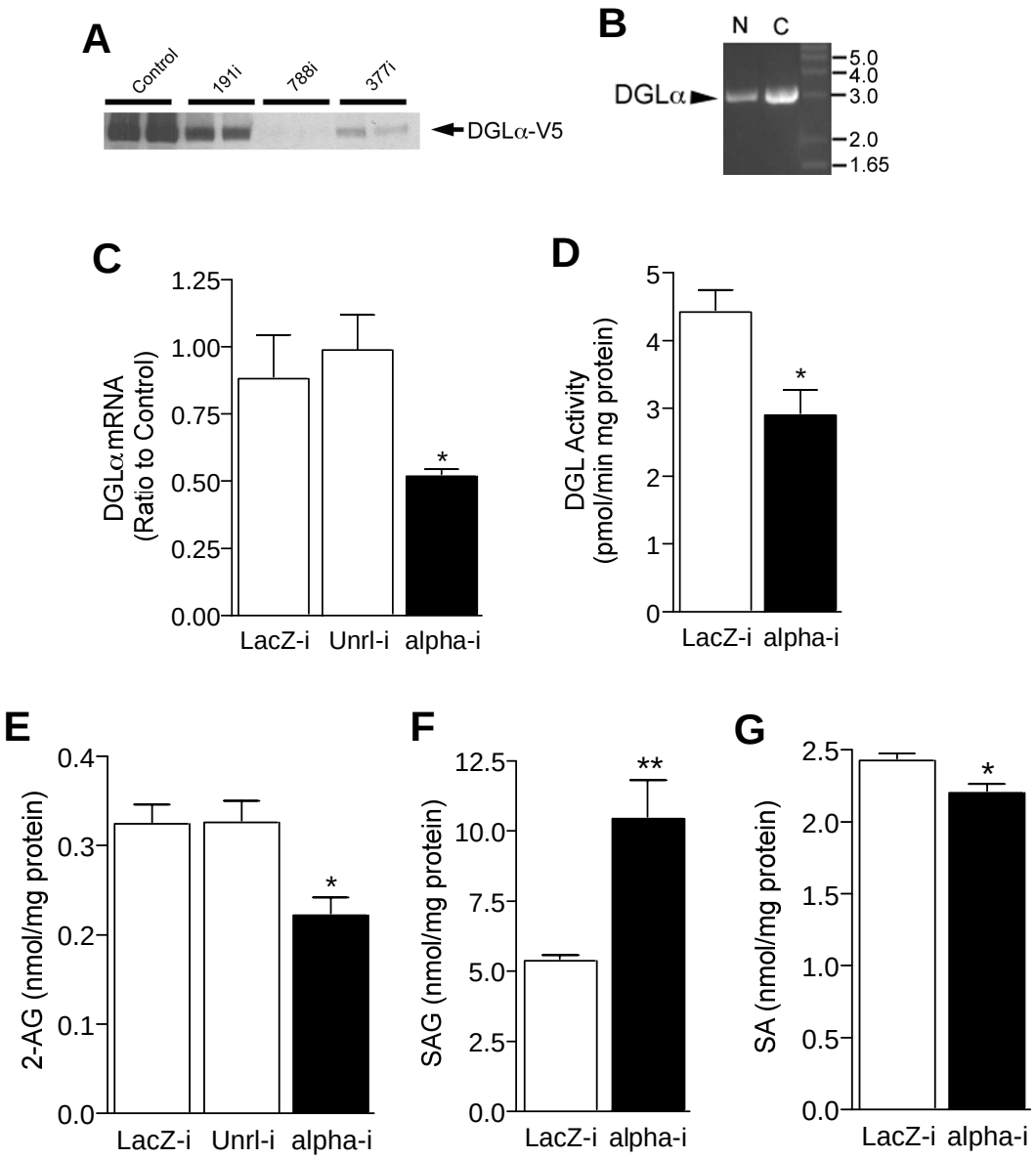

Fig 3

Molecular Pharmacology Fast Forward. Published on June 21, 2007 as DOI: 10.1124/mol.107.037796
This article has not been copyedited and formatted. The final version may differ from this version.

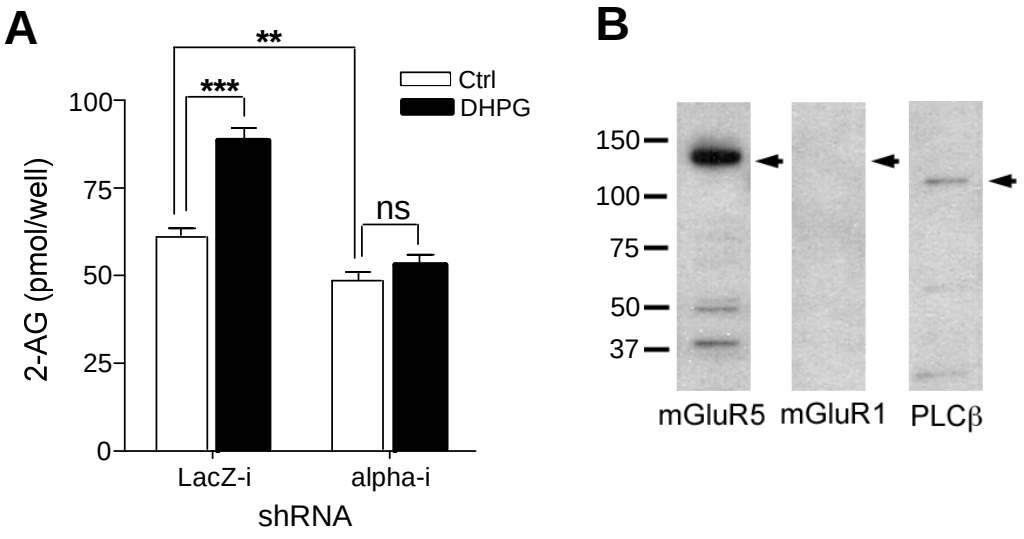

Fig 4

Molecular Pharmacology Fast Forward. Published on June 21, 2007 as DOI: 10.1124/mol.107.037796
This article has not been copyedited and formatted. The final version may differ from this version.

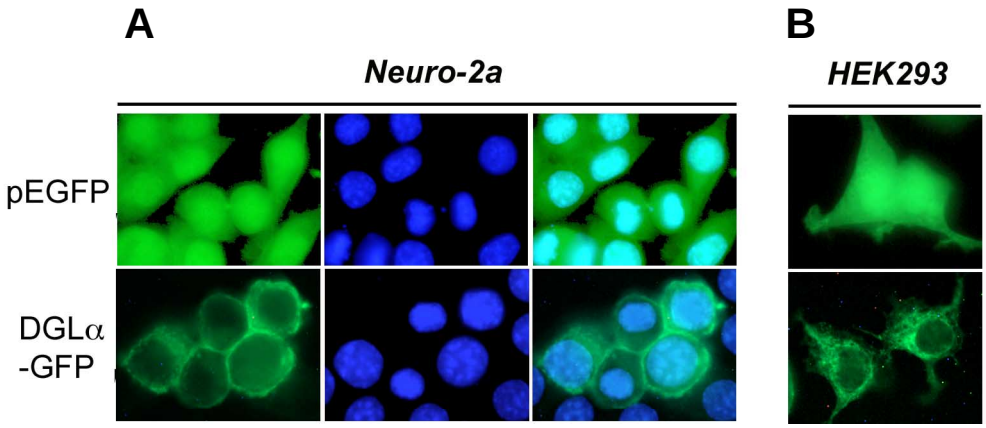

Fig 5

Molecular Pharmacology Fast Forward. Published on June 21, 2007 as DOI: 10.1124/mol.107.037796
This article has not been copyedited and formatted. The final version may differ from this version.

A

cDNA	Sequence
	********
DGLα -Human	KPPRLFAG (971-978)
-Mouse	KPPRLFAG (973-980)
-Rat	KPPRLFAG (973-980)
mGluR1aR (r)	TPPSPFRD (1145-1152)
mGluR5R (r)	TPPSPFRD (1123-1130)
IP3R (h)	NPPKKFRD (48-55)
RyR (h)	RPPHHFSA (1771-1778)

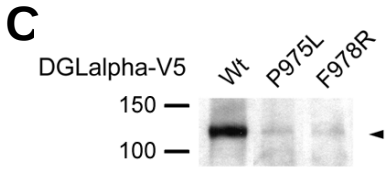

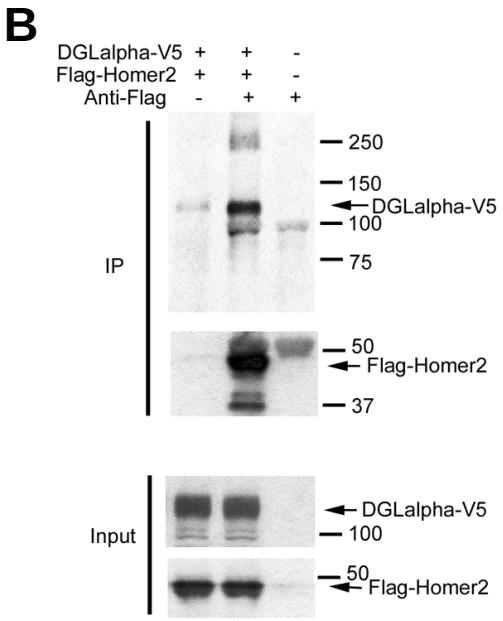

Fig 6

Molecular Pharmacology Fast Forward. Published on June 21, 2007 as DOI: 10.1124/mol.107.037796
This article has not been copyedited and formatted. The final version may differ from this version.

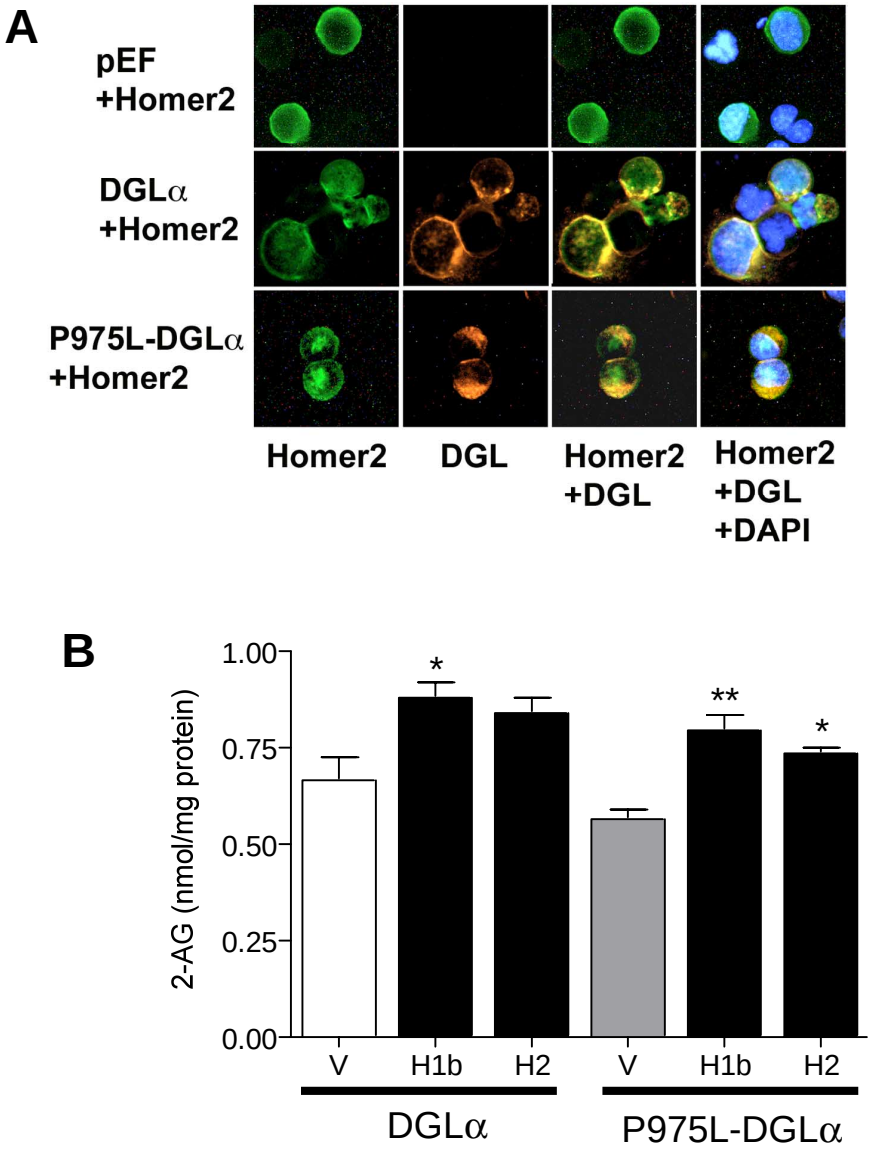

Fig 7